Title: The Application of ATR-FTIR Spectroscopy and Multivariate Data Analysis to Study Drug Crystallisation in the Stratum Corneum

Authors and affiliations: Choon Fu Goh[a], Duncan Q. M. Craig[b], Jonathan Hadgraft[b], Majella E. Lane[b]

[a]School of Pharmaceutical Sciences, Universiti Sains Malaysia, Penang 11800, Malaysia

[b]Department of Pharmaceutics, UCL School of Pharmacy, 29-39 Brunswick Square, London WC1N 1AX, United Kingdom

Corresponding author: Choon Fu Goh

<u>First author</u>

Given name: Choon Fu **Last name:** Goh

Affiliation: School of Pharmaceutical Sciences, Universiti Sains Malaysia, Penang 11800, Malaysia

Email: gohchoonfu@hotmail.com

<u>Second author</u>

Given name: Duncan **Last name:** Craig

Affiliation: Department of Pharmaceutics, UCL School of Pharmacy, 29-39 Brunswick Square, London WC1N 1AX, United Kingdom

Email: duncan.craig@ucl.ac.uk

<u>Third author</u>

Given name: Jonathan **Last name:** Hadgraft

Affiliation: Department of Pharmaceutics, UCL School of Pharmacy, 29-39 Brunswick Square, London WC1N 1AX, United Kingdom

Email: jonathan.hadgraft@btinternet.com

Fourth author

Given name: Majella **Last name:** Lane

Affiliation: Department of Pharmaceutics, UCL School of Pharmacy, 29-39 Brunswick Square, London WC1N 1AX, United Kingdom

Email: majella.lane@btinternet.com

ABSTRACT

Drug permeation through the intercellular lipids, which pack around and between corneocytes, may be enhanced by increasing the thermodynamic activity of the active in a formulation. However, this may also result in unwanted drug crystallisation on and in the skin. In this work, we explore the combination of ATR-FTIR spectroscopy and multivariate data analysis to study drug crystallisation in the skin.

Ex vivo permeation studies of saturated solutions of diclofenac sodium (DF Na) in two vehicles, propylene glycol (PG) and dimethyl sulphoxide (DMSO), were carried out in porcine ear skin. Tape stripping and ATR-FTIR spectroscopy were conducted simultaneously to collect spectral data as a function of skin depth. Multivariate data analysis was applied to visualise and categorise the spectral data in the region of interest (1700 – 1500 cm^{-1}) containing the carboxylate (COO^-) asymmetric stretching vibrations of DF Na.

Spectral data showed the redshifts of the COO^- asymmetric stretching vibrations for DF Na in the solution compared with solid drug. Similar shifts were evident following application of saturated solutions of DF Na to porcine skin samples. Multivariate data analysis categorised the spectral data based on the spectral differences and drug crystallisation was found to be confined to the upper layers of the skin.

This proof-of-concept study highlights the utility of ATR-FTIR spectroscopy in combination with multivariate data analysis as a simple and rapid approach in the investigation of drug deposition in the skin. The approach described here will be extended to the study of other actives for topical application to the skin.

GRAPHICAL ABSTRACT

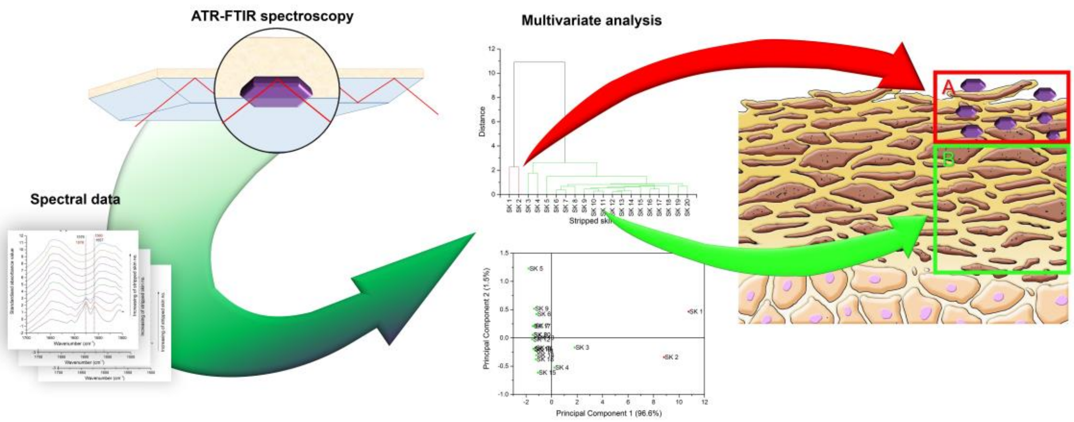

KEY WORDS

Stratum corneum; Crystallisation; ATR-FTIR; Multivariate data analysis, Porcine skin

CHEMICAL COMPOUNDS STUDIED IN THIS ARTICLE

Diclofenac sodium (PubChem CID: 5018304); Dimethyl sulphoxide (PubChem CID: 679); Propylene glycol (PubChem CID: 1030)

ABBREVIATION

ATR-FTIR	Attenuated total reflectance Fourier transform infrared
DF Na	Diclofenac sodium
DMSO	Dimethyl sulphoxide
HCA	Hierarchical cluster analysis
IR	Infrared
PC(s)	Principal component(s)
PCA	Principal component analysis
PG	Propylene glycol
PLM	Polarised light microscopy
SC	Stratum corneum

1. INTRODUCTION

Supersaturation is a passive enhancement strategy which may be used to promote drug penetration across the skin [1]. It is achieved by loading an excess amount of drug in a formulation so that it exceeds its solubility limit. As this method implicitly increases the thermodynamic activity of a molecule, this creates an unstable state of the active and may result in crystallisation on and in the skin. Once crystallisation is initiated, drug is “stranded” in the skin with a consequent reduction in flux. Santos and coworkers have previously suggested that drug crystallisation contributed to the lack of permeation enhancement observed for supersaturated oxybutynin and fentanyl formulations [2-4]. Solvent depletion was also proposed in these studies as the primary driving force for drug crystallisation in the skin. Saar *et al.* [5] showed the formation of ibuprofen crystals on excised mouse skin using simulated Raman scattering (SRS) imaging, following application of a solution of deuterated ibuprofen in propylene glycol (PG). More recently, Belsey *et al.* [6] observed large ibuprofen crystals on porcine skin 30 min post application of a saturated solution of ibuprofen in PG using the same imaging technique. However, actual location of crystals in the skin remains a limitation of SRS imaging as is the apparent requirement for deuteration of the active of interest.

Depending on the active of interest, infra-red spectroscopy may allow a distinction to be made between the solid and solution forms. A modification of IR, Attenuated Total Reflectance Fourier Transform IR (ATR-FTIR), has previously been used for simultaneous monitoring of skin permeation of actives and vehicle components [7-11]. Because of the complexity of the spectral datasets which are typically collected, multivariate data analysis is a very useful tool to study subtle differences in IR spectra. Hierarchical cluster analysis (HCA) and principal component analysis (PCA) have both been used to classify spectroscopic results based on their dissimilarity and variations [12].

Our approach in this proof-of-concept study is to demonstrate a rapid and simple experimental setup using ATR-FTIR spectroscopy to examine drug crystallisation in the skin. Simple formulations of diclofenac sodium (DF Na) in two different penetration enhancers – PG or dimethyl sulphoxide (DMSO) were applied to porcine skin samples. Diclofenac is a potent nonsteroidal anti-inflammatory drug (NSAID) for general treatment of pain and inflammation. It is usually formulated as salt forms such as diclofenac sodium or potassium as a strategy to improve the solubility and/or stability. Various approaches to enhance the skin penetration of diclofenac have been reviewed in a previous publication [13]. Santos et al. [2-4] previously suggested that PG may promote drug crystallisation in the skin and DMSO is also known to induce the formation of steroid reservoirs in the skin [14].

2. MATERIALS AND METHODS

2.1. Materials

Diclofenac sodium (DF Na) was purchased from AK Scientific Inc. (Union City, CA, US). PG and DMSO were obtained from Sigma-Aldrich (Gillingham, UK). Hydrochloric acid (1M) was obtained from Alfa Aesar (Ward Hill, MA, US). Sodium chloride and sodium hydroxide were supplied by VWR International Ltd. (Lutterworth, UK) and Fischer Scientific (Loughborough, UK). A Bradford protein assay kit was obtained from Sigma-Aldrich (Gillingham, UK). Scotch packaging tape (3M, St. Paul, MN, US) was obtained from a local stationery store. HPLC grade water, methanol, acetonitrile and trifluoroacetic acid (TFA) were obtained from Fischer Scientific

(Loughborough, UK). Full thickness porcine skin tissues were isolated from porcine ear skin obtained from a local abattoir and were stored at -20ºC before use.

2.2. Preparation of saturated solutions of DF Na

Saturated solutions of DF Na were prepared by adding excess DF Na to PG and DMSO followed by agitation of the solutions in an oven for 48 h at 32 ± 1ºC [15, 16]. The solutions were centrifuged to obtain supernatant for solubility determination using HPLC.

2.3. *Ex vivo* permeation studies and tape stripping using porcine ear skin

An infinite dose (95 µL/cm^2) of the DF Na solution was applied to a delineated area of porcine ear skin (7.5 × 1.5 cm) for 1 h at room temperature. This dosing area is slightly larger than the dimensions of the ATR zinc selenide (ZnSe) crystal (7.2 × 1.0 cm^2). The area was not occluded in order to maximise the possibility of drug crystallisation. Gauze was cut to the same size of the dosing area before application of solutions to ensure no spreading beyond the delineated areas. After 1 h, the gauze was removed and the sites were gently wiped with dry tissues to remove excess solution before tape stripping. The skin was then held firmly using pins on a cork board overlaid with a piece of Parafilm® before tape stripping. The sequential removal of SC via tape stripping was carried out using Scotch packaging tape. A plastic template with a rectangular aperture (~8 × 2 cm^2) was used to ensure all crystals which might be present on the skin surface could be recovered from the sample site. Twenty sequential tapes were obtained in each set of experiments for the tape stripping procedure. The direction of tape removal was alternated in order to achieve more uniform stripping of the SC [17, 18]. This *ex vivo* tape stripping procedure was standardised in terms of intensity by using a 10 cm long lint roller (Primark, Reading, UK) and the speed of tape stripping was monitored to ensure reproducibility.

2.4. ATR-FTIR spectroscopy

2.4.1. Spectra collection for solid and solution forms of DF Na

A FTIR spectrometer (Tensor 27; Bruker Optics Ltd., Coventry, UK) with a Specac™ multi-bounce (25 reflection, 45º, refractive index of 2.40) ATR accessory (Specac Ltd., Orpington, UK) – ZnSe (7.2 × 1.0 cm^2), was used to collect the reference spectra for the solid form of DF Na (ethanolic paste), DF Na in PG (200 mg/mL) and DMSO (100 mg/mL). The ethanol paste of DF Na was prepared by mixing a minimal amount of ethanol with DF Na powder. This paste was then spread evenly on the ZnSe crystal and allowed to dry for about half an hour before collecting spectra [7]. For analysis of solutions, an aluminum slab was used to form a reservoir using vacuum grease. For each sample 32 scans were collected with a resolution of 4 cm^{-1} in the range of 4000 cm^{-1} to 600 cm^{-1}. The spectra collected were analysed using Opus software version 6.0 (Bruker Optics Ltd., Coventry, UK) and OriginPro 9.0.0 (OriginLab Corp., Northampton, MA, US).

2.4.2. Spectra collection during tape stripping

The ATR-FTIR spectrum of porcine ear skin as a control was obtained before application of DF Na solutions to ensure no chemical contamination. The skin was placed in contact with the ZnSe crystal (SC facing downward) with a constant pressure under a weight (100 mg) to establish close contact before spectral collection. After 1 h of application of the samples to the skin a further spectrum was collected before tape stripping. The subsequent FTIR spectra collection were carried out simultaneously with the tape stripping procedure. For every tape stripping step, FTIR spectra were collected for both the tape strip and stripped skin. In order to ensure good contact with the surface of the ZnSe crystal, the tape strip was adhered firmly (adhesive part facing down) and trapping of air was avoided. The stripped skin was placed in close contact with a constant pressure. The surface of the ZnSe crystal and its holder were cleaned with ethanol to avoid cross contamination between scans. Three replicates were conducted for each saturated solution. These steps were repeated for the control study without any treatment, and also for treatment with the neat solvents (95 µL/cm^2).

2.5. Polarised light microscopy (PLM)

Tape strips were observed using a polarised light microscope (Leica DM L52, Germany). The images were captured using an INFINITY2 digital camera and INFINITY2 software (Lumenera Corp., Ontario, Canada) at 5× magnification. Studio86 Design capture software (Lutterworth, UK) was used to collect the images.

2.6. Extraction and analysis of DF Na in the tapes

The content of DF Na was quantified from each tape strip by extraction in methanol overnight. The tape strip was cut into smaller pieces and placed in a 2 mL eppendorf tube containing 1 mL of methanol. A second extraction was carried out with an equal volume of methanol. The extracts were suitably diluted and analysed using HPLC. The extraction was performed in triplicate. The method was validated by spiking tape-stripped samples of untreated SC with known amounts of DF Na in PG or DMSO with more than 95% recovery (data not shown).

2.7. HPLC analysis

DF Na was quantified using an Agilent 1100 Series G1311A quaternary pump (Hewlett Packard, Santa Clara, CA, US), set at a flow rate of 1.2 mL/min, with a G1315B Diode Array Detector set at 277 nm. The stationary phase was a Shiseido Capcell Pak C_{18} 5 µm column (250 x 4.6 mm) (Tokyo, Japan) attached to a SecurityGuard™ guard column with C_{18} cartridge (Phenomenex, Macclesfield, UK). The mobile phase was 70% acetonitrile, 30% water and 0.1% TFA. Samples were injected via a 25 µL loop and the retention time was 4.8 min. The HPLC method was developed and validated according to the ICH guideline Q2(R1) [19]. The lower limits of detection and quantification for DF Na were 0.1 and 0.5 µg/mL, respectively.

2.8. Bradford protein assay

The protein content of porcine SC removed with each tape strip for untreated porcine skin was quantified using the Bradford protein assay (micro 2 mL assay protocol, Technical bulletin Catalog Number B6919). The Bradford protein assay is pH sensitive and the readings were clearly affected by the presence of PG or DMSO. The tape strips were cut into small pieces before transfer to 10 mL scintillation vials. A volume of 4 mL of 1 M sodium hydroxide solution was added to extract the protein. The amount of sodium hydroxide was four times the quantity previously used to extract protein from porcine SC for an area of ~ 4 cm^2 using D-Squame® and Corneofix® tapes [20]. These vials were then shaken at 37ºC for 1 h and sonicated for 30 – 60 min at room temperature to fully extract the proteins. A 500 µL aliquot of solution was transferred to 2 mL Eppendorf tubes and neutralised with an equal volume of 1M hydrochloric acid. After vortexing for 5 – 10 s, 250 µL of neutralised samples were transferred to 2 mL Eppendorf tubes and diluted with 750 µL 1M sodium chloride. Subsequently, 1 mL of Bradford reagent was added to each tube. The absorbance of the samples at 595 nm was determined at room temperature with a Biomate 3 UV/Vis Spectrophotometer (Thermo Spectronic, Rochester, NY, US). A blank tape served as a control and was extracted in a similar manner as for the tapes containing protein for each set of experiments. The protein content was determined based on a calibration curve developed using freshly prepared SC standard solutions in the concentration range 0 – 500 µg/mL [21]. In order to ensure all protein was solubilised in sodium hydroxide after one extraction, the tapes were removed for a second extraction with sodium hydroxide and quantified using the same method.

2.9. Multivariate data analysis

The FTIR spectra in the 1700 – 1500 cm^{-1} region were selected for study because this range contains characteristic bands of the diclofenac molecule, namely carboxylate (COO^-) asymmetric stretching vibrations. Preprocessing of spectral data was performed by standardisation (normalisation to *z* score). Normalisation is important for dissimilarity or distance measurement such as the Euclidean distance which is sensitive to the differences within the magnitude or scales of the variables [22]. It also helps to compensate for the differences in sample quantity or a different optical pathlength and improves accuracy and efficiency of the data models [23-25]. Hierarchical cluster analysis (HCA) and principal component analysis (PCA) were performed using OriginPro 9.0.0 (OriginLab Corp., Northampton, MA, US). The dissimilarity of spectra in HCA was measured by the Euclidean distance to generate a dendrographic classification. PCA was represented by a score plot and the corresponding PCs which explain more than 90% of total variance.

3. RESULTS

3.1. Saturated solubility of DF Na

The saturated solubility of DF Na in PG at 32ºC was determined to be 386 ± 18 mg/mL and the corresponding value in DMSO was 149 ± 9 mg/mL. The solubility of DF Na in DMSO is consistent with the concentration estimated from the solubility graph of DF Na (~ 165 mg/g) reported by Žilnik *et al.* [26].

3.2. ATR-FTIR spectra of DF Na in solid and solution forms

The ATR-FTIR spectrum of DF Na (ethanolic paste) is shown in Figure 1A. The carboxylate (COO^-) functional group shows asymmetric stretching vibrations in the 1610 – 1560 cm^{-1} region. The presence of an aromatic ring also contributes to the C=C stretching vibrations near 1500 – 1400 cm^{-1}. A broad absorption band around 3700 – 3000 cm^{-1} is attributed to N–H and O–H stretching vibrations.

Figure 1B shows the standardised ATR-FTIR spectra of DF Na in different forms – solid ethanolic paste, solutions of DF Na in PG (200 mg/mL) or DMSO (100 mg/mL). The ATR-FTIR spectra for unsaturated drug solutions were collected for comparison as the saturated drug solutions tended to crystallise rapidly. When DF Na is dissolved in the selected penetration enhancers, the ATR-FTIR spectra are similar to those of the penetration enhancers alone apart from the 1700 – 1500 cm^{-1} region. Peak shifts were observed for the COO^- asymmetric stretching vibrations, from 1576 cm^{-1} to 1578 cm^{-1} and from 1557 cm^{-1} to 1560 cm^{-1}, when DF Na was dissolved in PG (Figure 1B I). However, these peak shifts were not evident when DF Na was dissolved in DMSO. A new peak shift was observed from 1557 cm^{-1} to 1558 cm^{-1} and the shoulder of the peak at 1576 cm^{-1} was split as an additional peak at 1587 cm^{-1} (Figure 1B II). These changes enable the differentiation of DF Na when it is fully dissolved in or is in the crystalline form. Therefore, ATR-FTIR spectra in the 1700 – 1500 cm^{-1} range were selected for examination following application of DF Na solutions to skin.

3.3. ATR-FTIR spectra for tape stripping work

Tape stripping on untreated skin was conducted concurrently with spectral collection for both stripped skin and tape strips containing SC. The standardised ATR-FTIR spectra in Figure 2 show the amide I and II bands of the SC. However, there are additional peaks in tape strips containing SC from the C=C stretching vibrations of the tape (polypropylene) near the 1650 – 1600 cm^{-1} region.

With the application of neat PG or DMSO, the 1700 – 1500 cm^{-1} region was unaffected, except for peaks associated with protein (Figure 2). The amide I band provides information about the secondary structure of proteins in the skin [27]. An α-helix protein conformation gives rise to a band in the range of 1647 – 1657 cm^{-1} while a β-sheet structure is associated with the 1621 – 1640 cm^{-1} and 1671 – 1679 cm^{-1} regions [28]. A shoulder near 1620 – 1630 cm^{-1} was observed for both PG- and DMSO-treated samples. This additional new feature suggested the formation of β-sheet secondary protein structures [29, 30]. Modification of SC protein from the α-helix to the β-sheet conformation by both PG and DMSO has also been reported by several researchers [31-34].

Changes in the amide bands of the SC were also evident following application of DF Na solutions (Figure 3). A new feature in these spectra was the COO^- asymmetric stretching vibrations which indicate the presence of DF Na. This was observed at 1576 cm^{-1} and 1557 cm^{-1} which represents the solid form of DF Na, following application of the saturated solution of DF Na in PG (Figure 3). However, weaker COO^- asymmetric stretching vibrations were observed following the application of the solution of DF Na in DMSO. This may be related to the lower solubility of DF Na in DMSO compared with PG with no major changes in the ATR-FTIR spectra. In this case, appearance of a peak at 1558 cm^{-1} in the region of COO^- asymmetric stretching vibrations suggested the presence of the DF Na in solution. Considering the COO^- asymmetric stretching vibrations indicating the DF Na in the solution under the influence of DMSO, multivariate data analysis was applied to further differentiate the spectra following application of saturated solutions of DF Na in PG only.

3.4. Multivariate data analysis

Multivariate data analysis was applied to deconvolute the standardised spectral data in the 1700 – 1500 cm^{-1} region. The statistical analysis was performed on the spectral data collected from stripped skin as there was strong interference from tape strips, especially in deeper skin layers. The spectra collected immediately after application of saturated solutions were excluded in this analysis (especially in principal component analysis, PCA) because the intensity of the COO^- asymmetric stretching vibrations of DF Na was much higher than that of the amide peaks. This might reflect the presence of drug crystals on the skin surface, sandwiched between the ZnSe crystal and the skin, during spectral data collection; this would hinder the evanescent wave from reaching the skin. The presence of these spectra may also contribute to a reduced correlation for other datasets.

Figure 4 shows dendrographic classifications (hierarchical cluster analysis, HCA), score plots and the first two principal components, PCs (PCA) for the standardised ATR-FTIR spectra in the 1700 – 1500 cm^{-1} region, for stripped skin, after application of DF Na in PG. The dissemblance of each data set allows the clustering of the spectral data based on the Euclidean distance as represented in the dendrogram, where two distinctive clusters were observed. In these dendrograms, the first two observations, in most cases, were clearly distinguished from each other, showing a large difference in Euclidean distances between them (Figure 4A). This was also in agreement with the two-dimensional score plots obtained from PCA as shown in the same figure (Figure 4B). In PCA analysis, the first two PCs described more than 95% of the total variance observed. PC1 contains the highest source of variance for the data elements and completely describes the presence of DF Na as represented by the COO^- asymmetric stretching vibrations (Figure 4C). Spectral data with significant spectral variations along PC1 were represented by the first cluster identified in the HCA. On the other hand, PC2, with the second highest variance, describes largely porcine SC and in part, background noise. This characterised the spectral data in the second cluster described in the HCA.

Data clusters may be represented by a block model of SC with two different zones (Figure 5). This diagram contains two zones: zone A – saturated solutions have permeated and crystals are present, and zone B – saturated solutions have permeated with minimal or no drug crystal formation. Zone A represents the spectral data grouped in the first cluster (red) in HCA and the first PC in PCA. This zone shows the presence of the COO^- vibrations associated with solid DF Na. The second zone (B) is similar to the ATR-FTIR spectra of the SC (stripped skin) where there is no detection of DF Na or only to a minimal extent. Zone B contains the spectral data as defined in the second cluster (green) in HCA and the second PC in PCA.

3.5. Polarised light microscopy (PLM)

Figure 6 shows the PLM images of representative tape strips after application of saturated solutions of DF Na in PG and DMSO. Drug crystals were found to be small and abundant with scattering on the first few tape strips. However, crystals were largely unobserved in the deeper layers of the SC (as evaluated using tape strip number). Nevertheless, these PLM images were consistent with evidence of drug crystallisation in the SC from the ATR-FTIR spectroscopy and multivariate data analysis.

3.6. Depth profiles of DF Na in porcine ear skin

The presence of DF Na in porcine ear skin was evaluated by extraction. Figure 7 shows the amount of DF Na extracted from tape strips following application of DF Na in PG or DMSO. Despite a large concentration difference in the initial tapes, the remaining tapes contained comparable amounts of drug, irrespective of the solvent. In these depth profiles, the amount of DF Na was found to be higher for PG, especially for the first few tapes. The total amount of DF Na extracted from 20 tape strips after application of DF Na in PG was determined to be 5.0 ± 1.2 μg/cm^2, almost twice the amount determined for DMSO (2.6 ± 0.5 μg/cm^2). This probably reflects the higher saturated solubility of DF NA in PG and is in good agreement with the results from the ATR-FTIR spectroscopic and microscopic imaging studies.

3.7. Bradford protein assay

The protein content of untreated porcine SC on tape strips was estimated using the Bradford protein assay. Knowing the tape stripped area (16 cm^2), the SC thickness which reflects the depth of the SC barrier may be calculated assuming a value of 1 g/cm^3 for SC density [35]. This value is also similar to that for human SC density (0.8 – 1.3 g/cm^3) reported by Anderson and Cassidy [36]. Figure 8 shows the average thickness of porcine SC removed by tape stripping. The total thickness of the SC removed from the 20 tape strips is estimated to be 7.7 ± 1.3 µm. Klang*, et al.* [20] estimated a total thickness of 7.96 ± 3.25 µm for SC removed from porcine skin using 80 – 130 tape strips but used a different type of tape.

An attempt to mixing penetration enhancers and the Bradford reagent resulted in a significant change in the colour. This indicates the interference of additives such as penetration enhancers with the Bradford protein assay. Thus, determination of protein content in the tape strips after treatment with penetration enhancers and formulations was not carried out. The SC thickness for the experiments involving these two vehicles is assumed to be the same as the untreated SC.

From the multivariate data analysis, it appears that drug crystals were present in *ex vivo* skin samples at a depth of 0.7 – 1.3 µm, which represents the superficial layers of the SC.

4. DISCUSSION

The phenomenon of drug crystallisation in percutaneous absorption has been suggested as one of the major factors compromising drug permeation over time. Several reports have shown the detection of drug crystals on mammalian skin but little is known about how the phenomenon actually happens in the skin [5, 6]. This study explored the combined abilities of (i) ATR-FTIR spectroscopy to detect drug crystals in skin samples and (ii) multivariate data analysis for differentiation of spectral characteristics descriptive of the physical state of the model drug. The important question addressed in this study is whether drug crystallisation does happen in the skin, specifically referring to the SC.

In this proof-of-concept study, drug crystals were found to be present in the superficial layers of the SC at a skin depth of 0.7 – 1.3 μm following topical application in PG. Even though drug extraction profiles showed the presence of drug in up to 20 tape strips, this observation does not differentiate crystalline DF Na and solubilised DF Na. Microscopic images, however, showed the presence of drug crystals on the tape strips for both saturated solution of DF Na in PG and DMSO but crystals were restricted to the first few layers of the SC. The microscopy observations are in line with the ATR-FTIR spectroscopic analysis of stripped skin for the application of DF Na in PG. The crystalline drug was detected only in the first two stripped skin samples using ATR-FTIR spectroscopy but not in the deeper layers of the SC. As drug is, in fact, expected to be present in small amounts in the deeper layers, the intensity of the COO^- asymmetric stretching vibrations for crystalline DF Na will be relatively weaker compared with other components of the SC (protein and lipid). Considering the relatively weaker COO^- asymmetric stretching vibrations in the deeper layers of the SC, the spectral data were subjected to multivariate data analysis to confirm the objective determination of the presence of theses vibrations in the spectra. Both hierarchical cluster analysis (HCA) and principal component analysis (PCA) successfully differentiated the spectral data into two distinct spectral groups with respect to the presence of COO^- asymmetric stretching vibrations of the crystalline DF Na. More importantly, this statistical analysis complements the subjective observation of COO^- asymmetric stretching vibrations present in the standardised spectra.

On the other hand, no crystalline drug was detected when applied in DMSO for all ATR-FTIR spectroscopic analyses despite the fact that the crystalline form of the drug was seen in the microscopic images in the first few tape strips. The absence of crystalline drug in the spectra following delivery in DMSO may be related to the sensitivity of the ATR-FTIR spectroscopy. From the drug extraction profiles (Figure 7), drug content in each tape strip following application in DMSO is generally below 0.5 µg/cm^2. In this case, one might speculate that any drug crystals present in a tape strip containing an amount of drug less than 0.5 µg/cm^2 are generally undetectable using ATR-FTIR spectroscopy. This might, therefore, be proposed as the lowest limit of detection of ATR-FTIR spectroscopy in this study with respect to the COO^- asymmetric stretching vibrations of crystalline DF Na. This would also agree with the results obtained for the application of drug solution in PG. The first two tape strips containing more than 0.5 µg/cm^2 of DF Na (Figure 7) showed the presence of COO^- asymmetric stretching vibrations of crystalline DF Na. The rest of the tape strips containing less than 0.5 µg/cm^2 of DF Na have no crystalline drug detected in the spectra, similar to all tape trips for the application of drug solution in DMSO. This result is also in line with the multivariate data analysis where the first two stripped skin samples were differentiated from the remaining samples based on these vibrations.

Deposition of solid drug in the skin as observed in the study is expected to prevent further penetration of drug deeper into the skin. The poor efficiency of topical formulations due to the unwanted drug crystallisation may be related to the drug reservoir formation in the skin [37]. The potential to create a drug reservoir in the skin was previously observed by other researchers but the mechanism of drug reservoir formation remains unknown [14, 38, 39]. The present study indicates that drug crystallisation in the skin may contribute to the formation of drug reservoir in the skin.

The investigation of drug crystallisation in the skin should be considered for future development and design of topical and transdermal formulations. It is important to ensure that formulations allow rapid lateral and vertical diffusion of drugs and partition into the intercellular spaces [37]. At present, the residence time of most excipients used in topical formulations and their interactions with drugs and the skin has not been widely reported. Recent reports on the real time measurement of drug permeation in the skin using Confocal Raman Spectroscopy may provide further insight into the fate of drug following topical and transdermal application [40-42].

5. CONCLUSIONS

Drug crystallisation is expected to have significant implications for delivery of actives from topical formulations as noted earlier. This proof-of-concept study outlined a rapid and simple approach using ATR-FTIR spectroscopy to identify drug crystallisation occurred in the skin for simple formulations of DF Na. We also applied multivariate data analysis in deconvolution of spectral data to visualise and differentiate the spectral data containing drug crystals from the skin. This study showed that the depth to which crystals could be found *ex vivo* was around 0.7 – 1.3 µm following topical application in a PG vehicle. Clearly, the technique may be applied to evaluate drug crystallisation behaviour for other actives used in topical formulations. We acknowledge that this is an *ex vivo* experimental set up but we will report validation of this approach *in vivo* with Confocal Raman Spectroscopy in future reports.

ACKNOWLEDGEMENT

The authors would like to thank the Ministry of Education Malaysia for funding a PhD studentship for Choon Fu Goh.

REFERENCES

[1] T. Higuchi, Physical chemical analysis of percutaneous absorption process from creams and ointments, Journal of the Society of Cosmetic Chemists, 11 (1960) 85-97.

[2] P. Santos, A.C. Watkinson, J. Hadgraft, M.E. Lane, Oxybutynin permeation in skin: The influence of drug and solvent activity, International Journal of Pharmaceutics, 384 (2010) 67-72.

[3] P. Santos, A.C. Watkinson, J. Hadgraft, M.E. Lane, Enhanced permeation of fentanyl from supersaturated solutions in a model membrane, International Journal of Pharmaceutics, 407 (2011) 72-77.

[4] P. Santos, A.C. Watkinson, J. Hadgraft, M.E. Lane, Influence of penetration enhancer on drug permeation from volatile formulations, International Journal of Pharmaceutics, 439 (2012) 260-268.

[5] B.G. Saar, L.R. Contreras-Rojas, X.S. Xie, R.H. Guy, Imaging drug delivery to skin with stimulated Raman scattering microscopy, Molecular Pharmaceutics, 8 (2011) 969-975.

[6] N.A. Belsey, N.L. Garrett, L.R. Contreras-Rojas, A.J. Pickup-Gerlaugh, G.J. Price, J. Moger, R.H. Guy, Evaluation of drug delivery to intact and porated skin by coherent Raman scattering and fluorescence microscopies, Journal of Controlled Release, 174 (2014) 37-42.

[7] W. Russeau, J. Mitchell, J. Tetteh, M.E. Lane, J. Hadgraft, Investigation of the permeation of model formulations and a commercial ibuprofen formulation in Carbosil® and human skin using ATR-FTIR and multivariate spectral analysis, International Journal of Pharmaceutics, 374 (2009) 17-25.

[8] W.J. McAuley, K.T. Mader, J. Tetteh, M.E. Lane, J. Hadgraft, Simultaneous monitoring of drug and solvent diffusion across a model membrane using ATR-FTIR spectroscopy, European Journal of Pharmaceutical Sciences, 38 (2009) 378-383.

[9] W.J. McAuley, M.D. Lad, K.T. Mader, P. Santos, J. Tetteh, S.G. Kazarian, J. Hadgraft, M.E. Lane, ATR-FTIR spectroscopy and spectroscopic imaging of solvent and permeant diffusion across model membranes, European Journal of Pharmaceutics and Biopharmaceutics, 74 (2010) 413-419.

[10] W.J. McAuley, S. Chavda-Sitaram, K.T. Mader, J.Tetteh, M.E. Lane, J. Hadgraft, The effects of esterified solvents on the diffusion of a model compound across human skin: An ATR-FTIR spectroscopic study, International Journal of Pharmaceutics, (2013).

[11] M. Dias, J. Hadgraft, S.L. Raghavan, J. Tetteh, The effect of solvent on permeant diffusion through membranes studied using ATR-FTIR and chemometric data analysis, Journal of Pharmaceutical Sciences, 93 (2004) 186-196.

[12] D. Naumann, H. Fabian, P. Lasch, FTIR spectroscopy of cells, tissues and body fluids, in: A. Barth, P.I. Haris (Eds.) Biological and Biomedical Infrared Spectroscopy, IOS Press BV, Amsterdam, 2009, pp. 324-349.

[13] C.F. Goh, M.E. Lane, Formulation of diclofenac for dermal delivery, International Journal of Pharmaceutics, 473 (2014) 607-616.

[14] R.B. Stoughton, Dimethylsulfoxide (DMSO) induction of a steroid reservoir in human skin, Archives of Dermatology, 91 (1965) 657-660.

[15] R.M. Watkinson, C. Herkenne, R.H. Guy, J. Hadgraft, G. Oliveira, M.E. Lane, Influence of ethanol on the solubility, ionization and permeation characteristics of ibuprofen in silicone and human skin, Skin Pharmacology and Physiology, 22 (2009) 15-21.

[16] G. Oliveira, J. Hadgraft, M.E. Lane, The influence of volatile solvents on transport across model membranes and human skin, International Journal of Pharmaceutics, 435 (2012) 38-49.

[17] N. Sekkat, Y.N. Kalia, R.H. Guy, Biophysical study of porcine ear skin *in vitro* and its comparison to human skin *in vivo*, Journal of Pharmaceutical Sciences, 91 (2002) 2376-2381.

[18] D.A. Weigand, J.R. Gaylor, Removal of stratum corneum *in vivo*: An improvement on the cellophane tape stripping technique, Journal of Investigative Dermatology, 60 (1973) 84-87.

[19] ICH, Validation of Analytical Procedures: Text and Methodology Q2(R1) FDA, 2005.

[20] V. Klang, J.C. Schwarz, A. Hartl, C. Valenta, Facilitating *in vitro* tape stripping: Application of infrared densitometry for quantification of porcine stratum corneum proteins, Skin Pharmacology and Physiology, 24 (2011) 256-268.

[21] F. Dreher, A. Arens, J.J. Hostýnek, S. Mudumba, J. Ademola, H.I. Maibach, Colorimetric method for quantifying human stratum corneum removed by adhesive-tape stripping, Acta Dermato-Venereologica, 78 (1998) 186-189.

[22] G. Milligan, M. Cooper, A study of standardization of variables in cluster analysis, Journal of Classification, 5 (1988) 181-204.

[23] P. Heraud, B.R. Wood, J. Beardall, D. McNaughton, Effects of pre-processing of Raman spectra on *in vivo* classification of nutrient status of microalgal cells, Journal of Chemometrics, 20 (2006) 193-197.

[24] K.-Z. Liu, K.S. Tsang, C.K. Li, R.A. Shaw, H.H. Mantsch, Infrared spectroscopic identification of β-Thalassemia, Clinical Chemistry, 49 (2003) 1125-1132.

[25] P. Lasch, Spectral pre-processing for biomedical vibrational spectroscopy and microspectroscopic imaging, Chemometrics and Intelligent Laboratory Systems, 117 (2012) 100-114.

[26] L.F. Žilnik, A. Jazbinšek, A. Hvala, F. Vrečer, A. Klamt, Solubility of sodium diclofenac in different solvents, Fluid Phase Equilibria, 261 (2007) 140-145.

[27] A.M. Kligman, E. Christophers, Preparation of isolated sheets of human stratum corneum, Archives of Dermatology, 88 (1963) 702-705.

[28] T.M. Greve, K.B. Andersen, O.F. Nielsen, Penetration mechanism of dimethyl sulfoxide in human and pig ear skin: An ATR–FTIR and near-FT Raman spectroscopic *in vivo* and *in vitro* study, Spectroscopy, 22 (2008).

[29] G. Zhang, D.J. Moore, C.R. Flach, R. Mendelsohn, Vibrational microscopy and imaging of skin: From single cells to intact tissue, Analytical and Bioanalytical Chemistry, 387 (2007) 1591-1599.

[30] M. Cotte, P. Dumas, M. Besnard, P. Tchoreloff, P. Walter, Synchrotron FT-IR microscopic study of chemical enhancers in transdermal drug delivery: Example of fatty acids, Journal of Controlled Release, 97 (2004) 269-281.

[31] R. Mendelsohn, M.E. Rerek, D.J. Moore, H.C. Chen, Infrared microspectroscopic imaging maps the spatial distribution of exogenous molecules in skin, Journal of Biomedical Optics, 8 (2003) 185-190.

[32] Z.U. Khan, I.W. Kellaway, Differential scanning calorimetry of dimethylsulphoxide-treated human stratum corneum, International Journal of Pharmaceutics, 55 (1989) 129-134.

[33] M.J. Clancy, J. Corish, O.I. Corrigan, A comparison of the effects of electrical current and penetration enhancers on the properties of human skin using spectroscopic (FTIR) and calorimetric (DSC) methods, International Journal of Pharmaceutics, 105 (1994) 47-56.

[34] Y. Takeuchi, H. Yasukawa, Y. Yamaoka, Y. Kato, Y. Morimoto, Y. Fukumori, T. Fukuda, Effects of fatty acids, fatty amines and propylene glycol on rat stratum corneum lipids and proteins *in vitro* measured by Fourier transform infrared/attenuated total reflection (FT-IR/ATR) spectroscopy, Chemical & Pharmaceutical Bulletin, 40 (1992) 1887-1892.

[35] R.O. Potts, M.L. Francoeur, The influence of stratum corneum morphology on water permeability, Journal of Investigative Dermatology, 96 (1991) 495-499.

[36] R.L. Anderson, J.M. Cassidy, Variations in physical dimensions and chemical composition of human stratum corneum, Journal of Investigative Dermatology, 61 (1973) 30-32.

[37] J. Hadgraft, M.E. Lane, Drug crystallization – implications for topical and transdermal delivery, Expert Opinion on Drug Delivery, 13 (2016) 817-830.

[38] F.D. Malkinson, E.H. Ferguson, Percutaneous absorption of hydrocortisone-4-C^{14} in two human subjects, Journal of Investigative Dermatology, 25 (1955) 281-283.

[39] C.H. Vickers, Existence of reservoir in the stratum corneum: Experimental proof, Archives of Dermatology, 88 (1963) 20-23.

[40] D. Mohammed, P.J. Matts, J. Hadgraft, M.E. Lane, *In vitro–in vivo* correlation in skin permeation, Pharmaceutical Research, 31 (2014) 394-400.

[41] R. Mateus, D.J. Moore, J. Hadgraft, M.E. Lane, Percutaneous absorption of salicylic acid – *in vitro* and *in vivo* studies, International Journal of Pharmaceutics, 475 (2014) 471-474.

[42] R. Mateus, H. Abdalghafor, G. Oliveira, J. Hadgraft, M.E. Lane, A new paradigm in dermatopharmacokinetics – Confocal Raman spectroscopy, International Journal of Pharmaceutics, 444 (2013) 106-108.

FIGURES

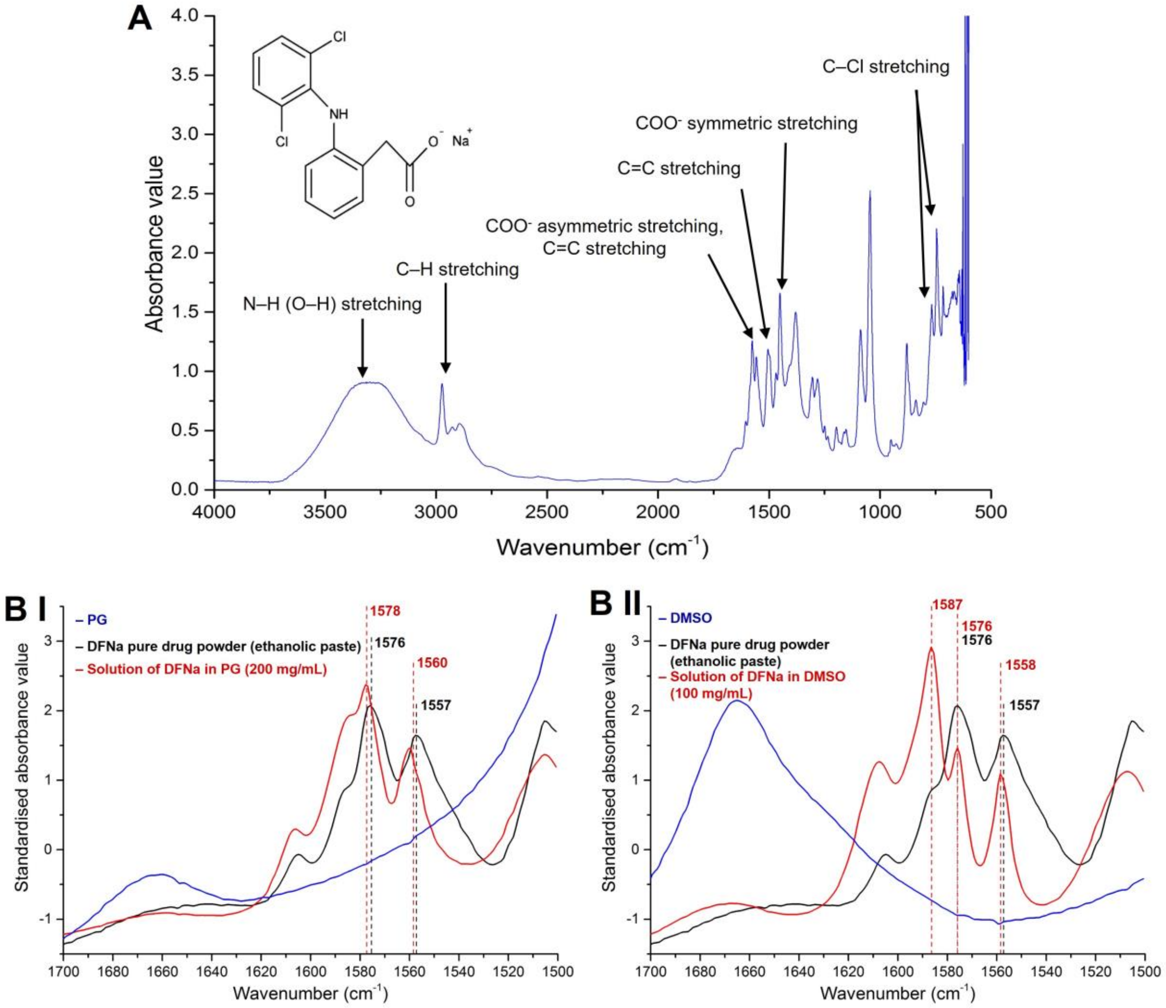

Figure 1 (A) ATR-FTIR spectrum of DF Na pure drug powder (ethanolic paste) and (B) standardised ATR-FTIR spectra (1700 – 1500 cm^{-1}) of DF Na pure drug powder (ethanolic paste), penetration enhancers – (I) PG and (II) DMSO and corresponding solutions of DF Na in PG (200 mg/mL) and DMSO (100 mg/mL)

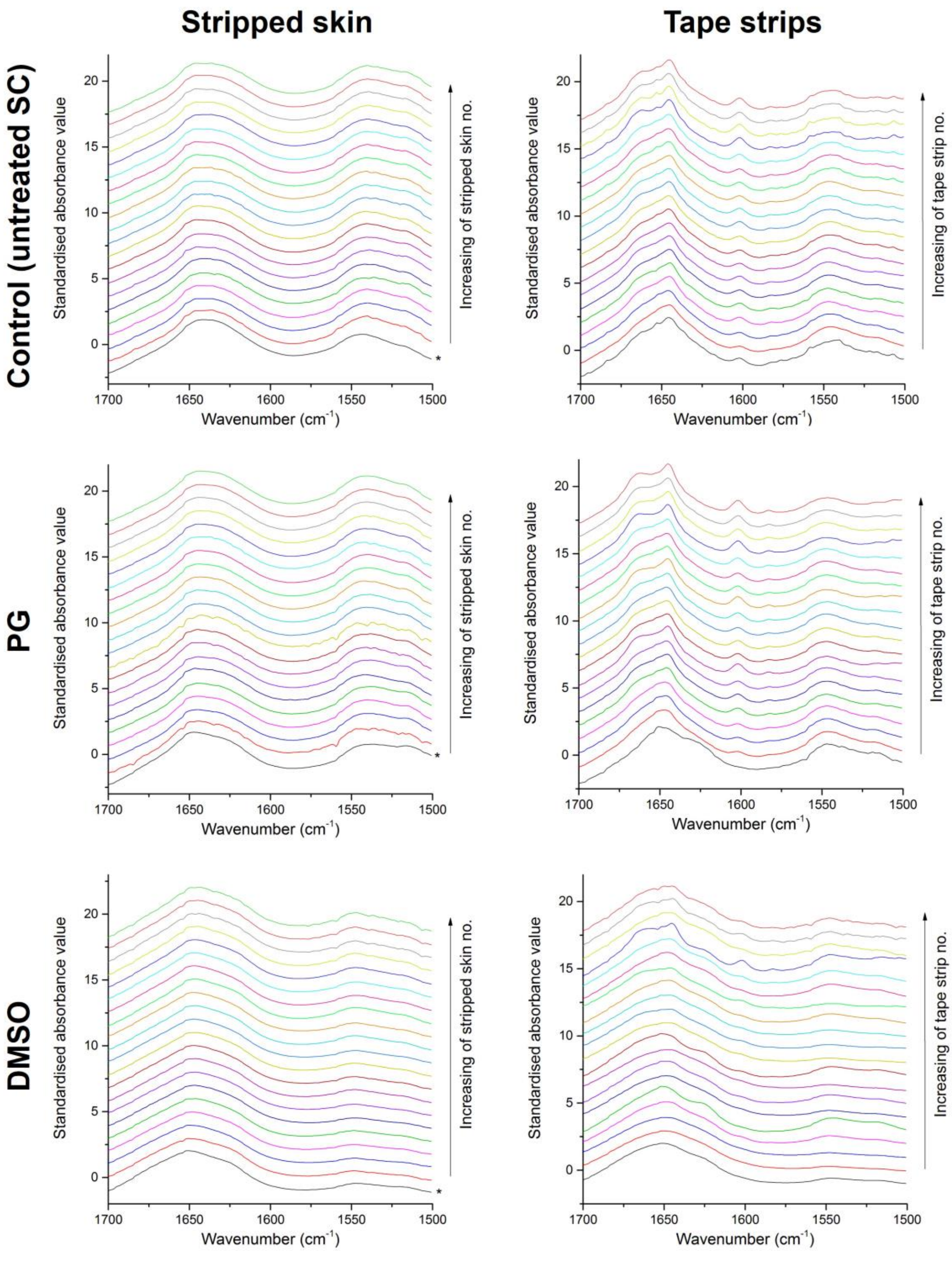

Figure 2 Standardised ATR-FTIR spectra of stripped skin and tape strips with and without any application of penetration enhancers (PG and DMSO). * represents the spectrum taken before tape stripping started.

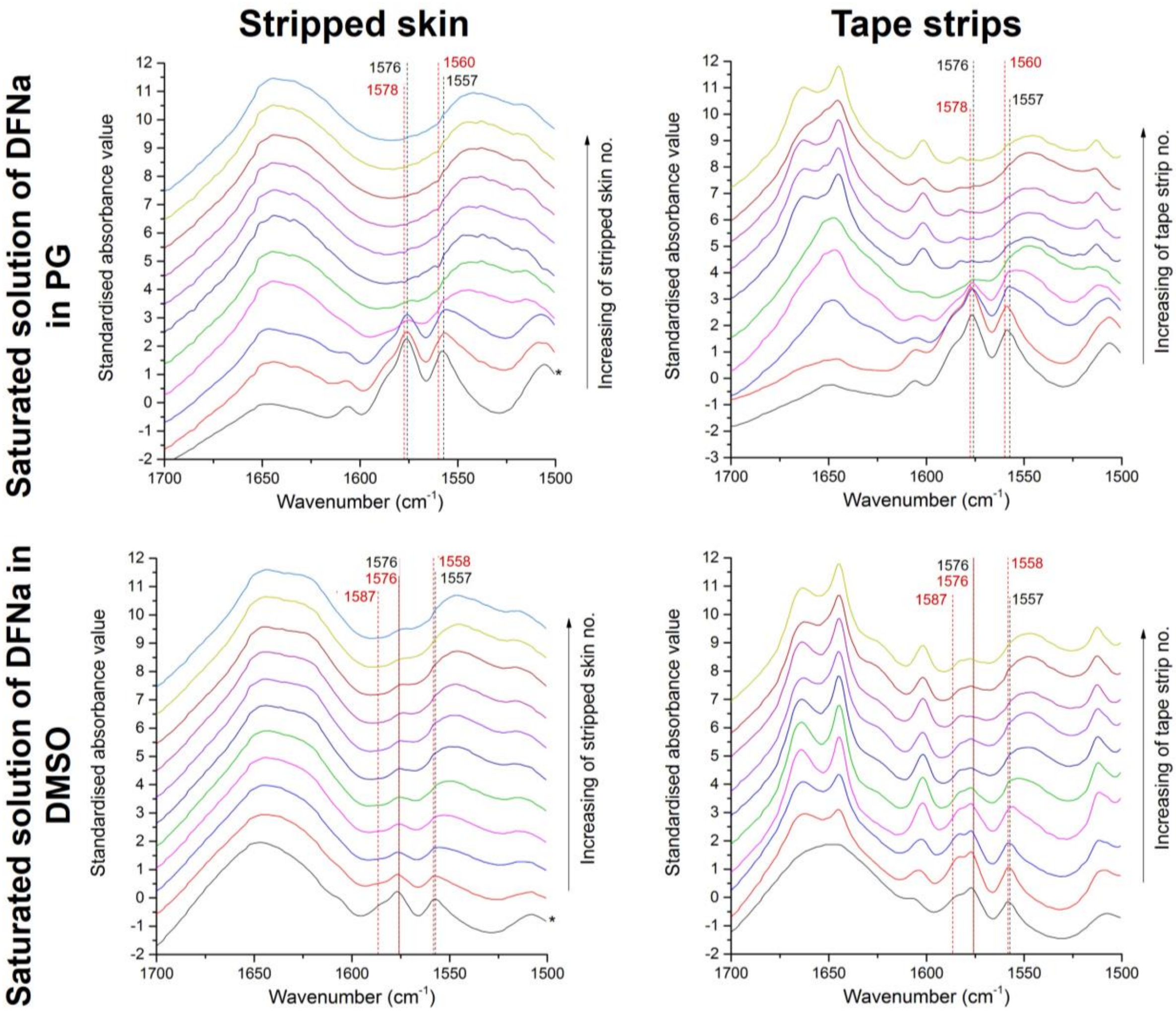

Figure 3 Standardised ATR-FTIR spectra of stripped skin and tape strips after application of the saturated solutions of DF Na in PG and DMSO (only the first ten spectra). * represents the spectrum taken before tape stripping started. Black and red dash lines are the wavenumbers recorded for the solid and solution form of DF Na, respectively.

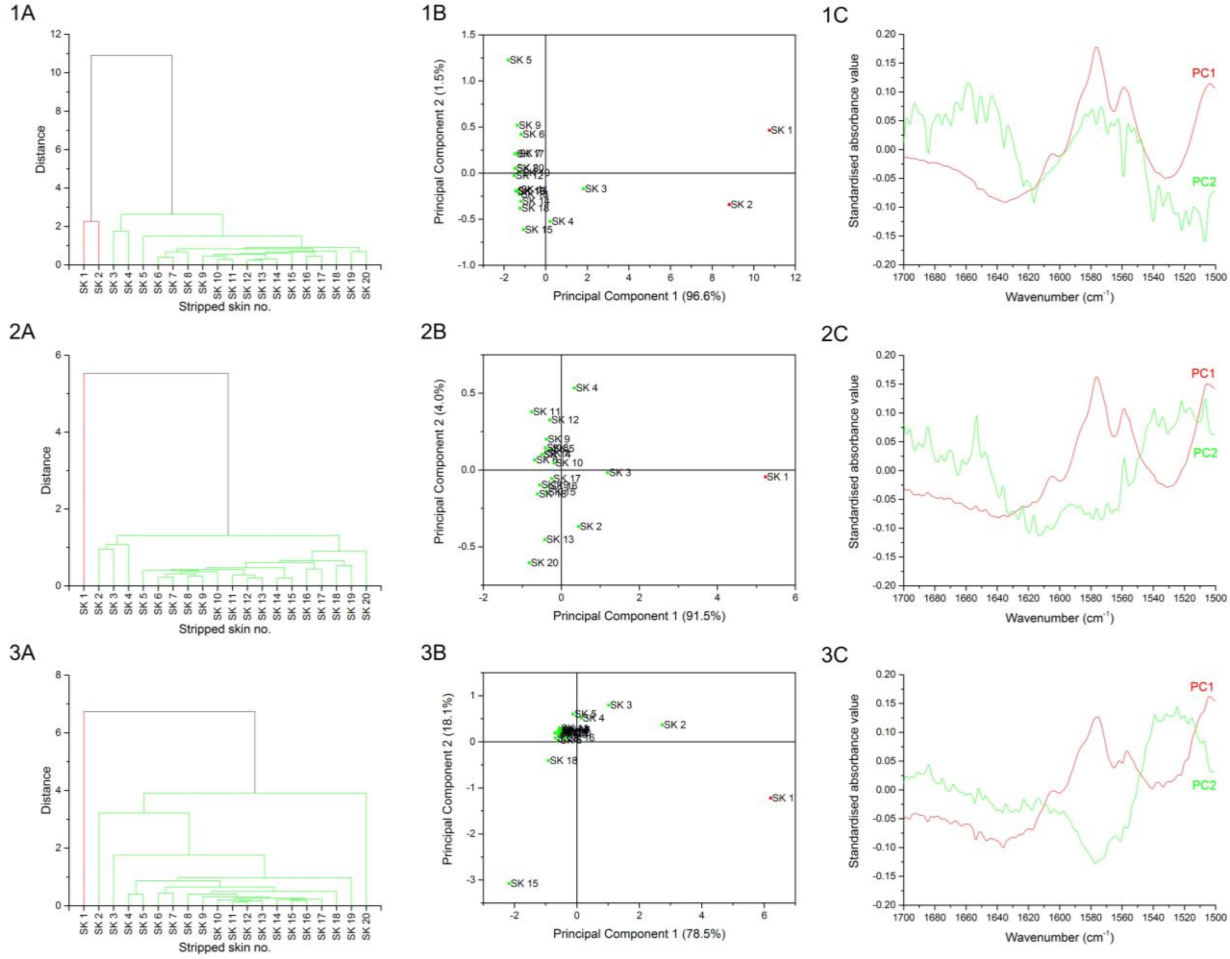

Figure 4 (A) Dendrographic classifications from HCA, (B) corresponding score plots and (C) first two PCs from PCA of standardised ATR-FTIR spectra between 1700 and 1500 cm^{-1} for stripped skin after application of the saturated solution of DF Na in PG. The percentage of variance in the data explained by each PC is shown in brackets on each axis of the score plots. The number on the top left denotes the number of replicates.

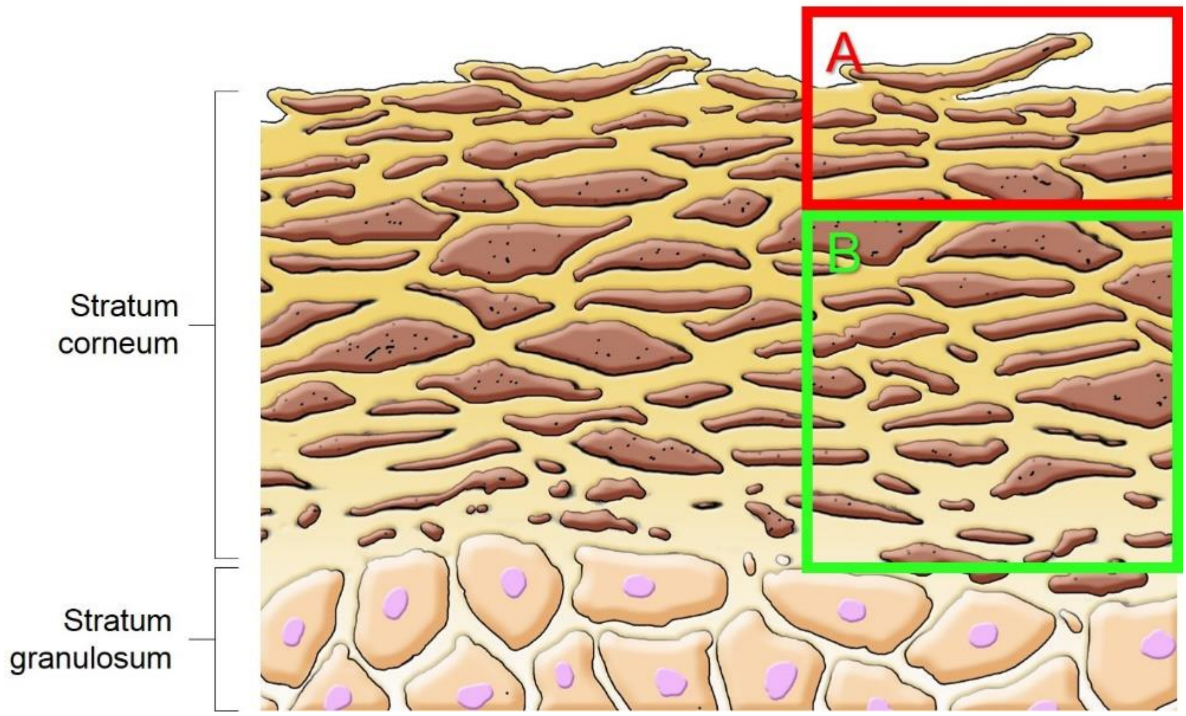

Figure 5 Zones of stratum corneum (SC) assigned using multivariate data analysis. Zone A (red): area where saturated solutions permeated with a high potential for drug crystallisaton; Zone B (green): area where saturated solutions permeated with minimal or no potential for drug crystallisation.

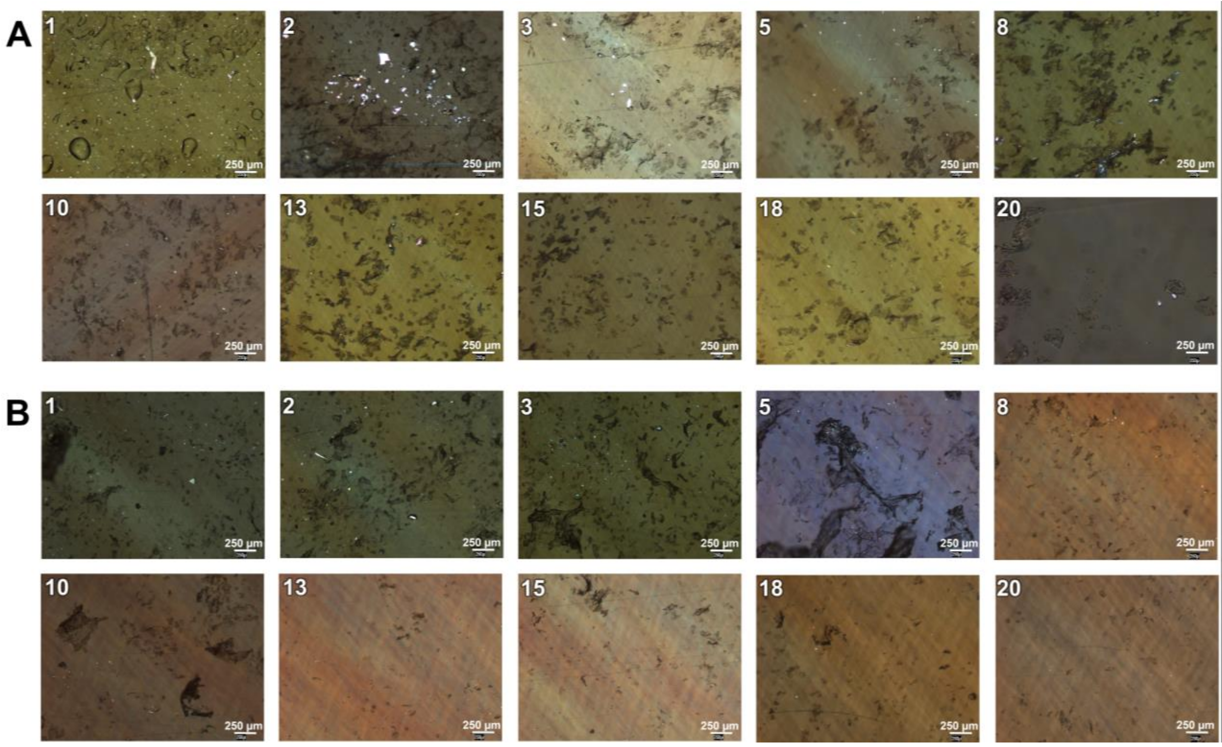

Figure 6 PLM images (5×) of representative tape strips obtained from the application of the saturated solutions of DF Na in (A) PG and (B) DMSO (scale bar: 250 µm). Number on the top left of each image indicates the tape strip number.

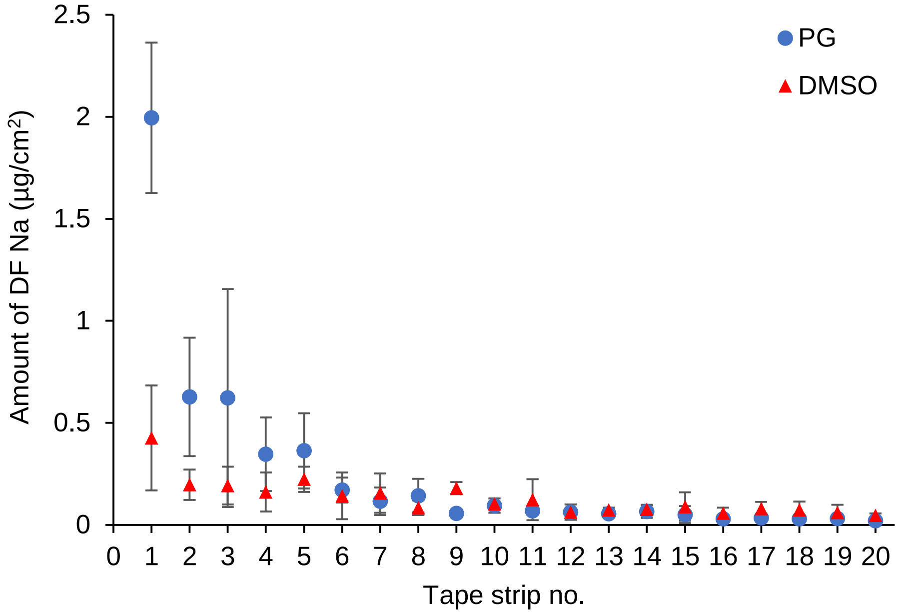

Figure 7 Amount of DF Na in the tape strips removed after 1 h *ex vivo* permeation of saturated solutions of DF Na in PG and DMSO (n = 3, mean ± SD)

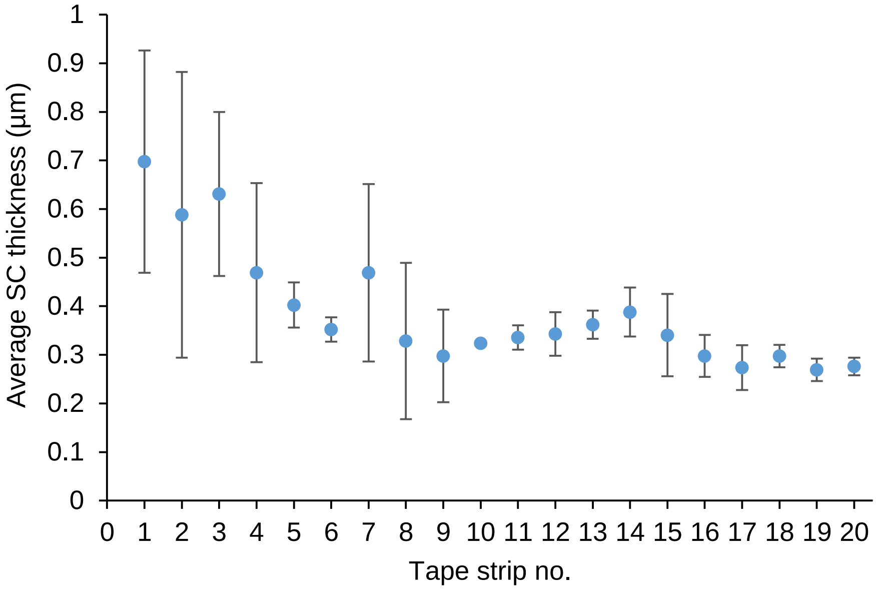

Figure 8 Average thickness of untreated porcine SC removed from 20 sequential tape strips (n = 3, mean ± SD)